Journal of Structural Geology, Vol. 14, No. 8/9, pp. 939 to 951, 1992
Printed in Great Britain

0191-8141/92 $05.00+0.00

Joint development in perturbed stress fields near faults

K. D. RAWNSLEY, T. RIVES and J.-P. PETIT

Laboratoire de géologie structurale, USTL, Place E. Bataillon, 34095 Montpellier Cédex, France

and

S. R. HENCHER and A. C. LUMSDEN

Department of Earth Sciences, University of Leeds, Leeds LS2 9JT, U.K.

(*Received* 28 *October* 1991; *accepted in revised form* 17 *April* 1992)

Abstract—Field evidence is presented for complex spatial and temporal perturbations of an otherwise systematic joint pattern around faults from well exposed faulted rock platforms.

Joints propagating in perturbed stress fields will curve to follow the directions of the stress field trajectories. A progressive change in joint direction is observed from unperturbed regions away from faults, to strongly perturbed zones adjacent to faults. This indicates that the joint pattern can reflect perturbations of the regional stress field around faults. In the examples, the stress field perturbations are probably due to points of high friction on the fault plane which concentrate stress and distort the stress field in the surrounding rock. The corresponding joints converge at these points and are sub-parallel to the fault along the remainder of the fault plane.

The possibility that a fault plane acts as a free surface contained within an elastic body is considered. In this situation the fault plane induces a rotation of the principal stress axes to become either perpendicular or parallel to the fault. The free surface model seems to explain the metre-scale curvature of joints in the vicinity of existing joints, but at the kilometre scale of a large fault plane the model becomes unrealistic unless the fault is open at the Earth's surface.

Two examples are investigated from the Lias of Great Britain; at Nash Point and Robin Hood's Bay. Both comprise sub-horizontal strata of relatively homogeneous lithology and bed thickness, which provide striking examples of joints developed near faults.

INTRODUCTION

ONE of the most striking characteristics of joint sets in many areas is their consistency in orientation, or gradual changes over extensive areas (Engelder & Geiser 1980). As a result, joints have been employed as regional palaeostress markers (Nickelsen & Hough 1967, Hancock 1985, Lorenz *et al.* 1991) assuming a straightforward relationship between the joints and the principal orientations of the regional stress field. Local abnormal patterns—directional deviations or complex superposition of several joint sets—are generally considered as anomalies of little interest and are neglected. Engelder (1987) stated that "random jointing develops when local folding and faulting have a complicated history ... The joint pattern that evolves under these circumstances is difficult or impossible to decipher". Recent advances have been made in the interpretation of perturbed joint patterns associated with folding (Dyer 1988) and in bending plate models (Rives & Petit 1990a) but many other local superpositions in complex joint patterns remain unexplained.

In this paper we consider that joints are mode I fractures. This point of view is widely accepted (Pollard & Aydin 1988) and is emphasized by the analogy between natural and analogue fracture patterns in brittle coating models (Rives & Petit 1990a, b, Rives 1991). In geological conditions this implies that joints form perpendicular to σ_3 and in the plane of σ_1 and σ_2 (where $\sigma_1 > \sigma_2 > \sigma_3$ are the principal effective stresses, and compressive stress is positive). The strike of each joint is the intersection of the σ_1 σ_2 plane with the horizontal plane and is thus the direction of maximum horizontal stress (σ_H) at the instant of joint formation.

Perturbations of the stress field around pre-existing fractures are known to exist and have been deduced from observation of the deviation of mesoscale stress-related structures such as stylolites and tension gashes (Rispoli 1981). Analogue and numerical models (Fletcher & Pollard 1981, Olson & Pollard 1989, Petit & Barquins 1990, Barquins & Petit, 1992, this issue) allow the description of the stress perturbations in the relatively simple cases of systems containing one or more fractures.

Since joints follow stress trajectories, stress field perturbations around pre-existing fractures (including joints and faults) may be associated with deviations in the orientation of younger joints. Localized joint pattern perturbations have been rarely described, however, Kazi (1982) showed a regional swing in joint orientation towards the North Craven Fault, northern England. Dyer (1988) and Rives & Petit (1991) showed changes in joint orientation due to folding, while Dyer (1988) and Simon *et al.* (1988) showed the effects of pre-existing joint sets on new joints. The large extent to which the stress field can be perturbed by even a simple defect suggests that most pre-existing faults must have perturbed younger joint development.

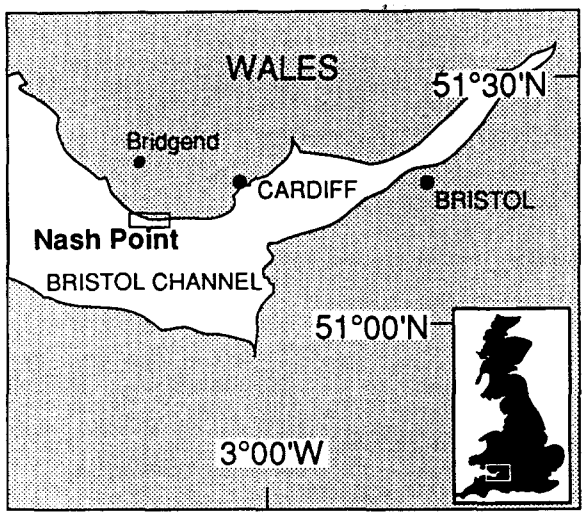

Fig. 1. Map indicating the position of Nash Point, U.K.

In addition to the effect of structures, joint development is also influenced by pore pressures (Secor 1965, Engelder & Lacazette 1990), mechanical rock properties (Suppe 1985), bed thicknesses (Ladeira & Price 1981, Narr & Suppe 1991), residual stress conditions (Reik 1973) and stress–strain magnitudes (Wu & Pollard 1991, Rives *et al.* 1992, this issue). Where such conditions for joint development are dissimilar on either side of a fault, the joint pattern may also vary. This type of joint pattern variation is not due to the fault plane itself and is not considered further.

In order to investigate stress field perturbations around pre-existing faults and their effect on joint development, we have selected two well exposed faulted sedimentary rock platforms. Each location consists of relatively homogeneous lithologies, bed thicknesses and with relatively minor folding. Joint patterns are described from Robin Hood's Bay along the Yorkshire Coast and from Nash Point along the South Wales coast. At both locations the complete joint pattern can be continuously observed over large distances, and changes in joint characteristics approaching the faults are obvious. Joint development models derived from analogue and numerical models are presented and compared.

GEOLOGICAL CONTEXTS AND JOINT NETWORKS

Nash Point: geological setting

Nash Point is located on the coast of South Wales, to the south of Bridgend (U.K. map reference SS 92 68, Fig. 1). On a regional scale the exposure is part of the E–W-trending Bristol Channel Basin which is an exhumed half graben of Mesozoic age contained between Palaeozoic terrains to the north and south (Brooks *et al.* 1988). The origin of the basin appears to be related to localized extensional reactivation of S-dipping Hercynian thrust zones and NNW–SSE strike-slip faults during the Permo-Triassic. This was followed by subsidence during the late Triassic and Jurassic (Van Hoorn 1987). Normal faulting occurred in response to N–S extension developed during the late Jurassic to early Cretaceous (Roberts 1989) which also reactivated the NNW–SSE-trending faults (Chadwick 1986, Holloway & Chadwick 1986, Brooks *et al.* 1988). Uplift of the basin in the early Tertiary produced sinistral strike-slip movement on the NNW–SSE faults and reactivation of the basement thrust (Roberts 1989). No kilometre-scale faults cut the rock platform at Nash Point. The nearest of the NNW–SSE faults is the Watchet–Lothelstone Fault (Stoneley 1982) which lies several kilometres to the west.

The rocks studied are also Liassic, forming both an extensive E–W-trending cliff line and a well exposed wave cut platform at its base. Beds comprise 1 m thick hard pale grey limestone and less thick shale horizons. The dip is close to horizontal and at low tides single beds are often exposed over many hundreds of square metres (Fig. 2a). A series of conjugate strike slip faults cut the sequence trending 010° ± 10° and 160° ± 10° with horizontal trace lengths often greater than the width of exposure (100–200 m). The faults are often incipient, and display sub-horizontal striations with very small vertical offsets implying only minor displacement.

Nash Point: joint network

At a distance of approximately 100 m from the faults the joint pattern consists of parallel and horizontally extensive (commonly over 100 m) joints striking 170° (Fig. 2a), which are spaced approximately 0.25 m apart (Rives *et al.* 1992). An orthogonal set rarely crosses the 170°-striking set.

In the vicinity of the faults this pattern is perturbed, with joint directions changing such that the joints curve towards points of convergence distributed irregularly along the fault planes. Points of joint convergence along fault planes have not been previously described. A typical, simple perturbation is shown in Fig. 2(b) with joints curving to become perpendicular to the fault at two points of convergence Fig. 2(c) with several centres of convergence and joints radial to each. The joint pattern in this example shows little relationship to the unperturbed pattern at Fig. 2(a), only 300 m to the west. The closely spaced faults and the large number of points of convergence on each fault has produced a complex superposition of the joint pattern.

Robin Hood's Bay: geological setting

Robin Hood's Bay (U.K. map reference NZ 9703) is located on the coast of North Yorkshire between Scarborough and Whitby (Fig. 3a). The rocks investigated are from the Jurassic Lower Lias Formation and are composed of sandy or micaceous shales inter-bedded with thin more resistant calcareous and siliceous harder beds ranging up to 1 m in thickness (Fox-Strangways & Barrow 1915). The bay exposes a dome feature with a centre off-shore and beds dipping inland at less than 5°.

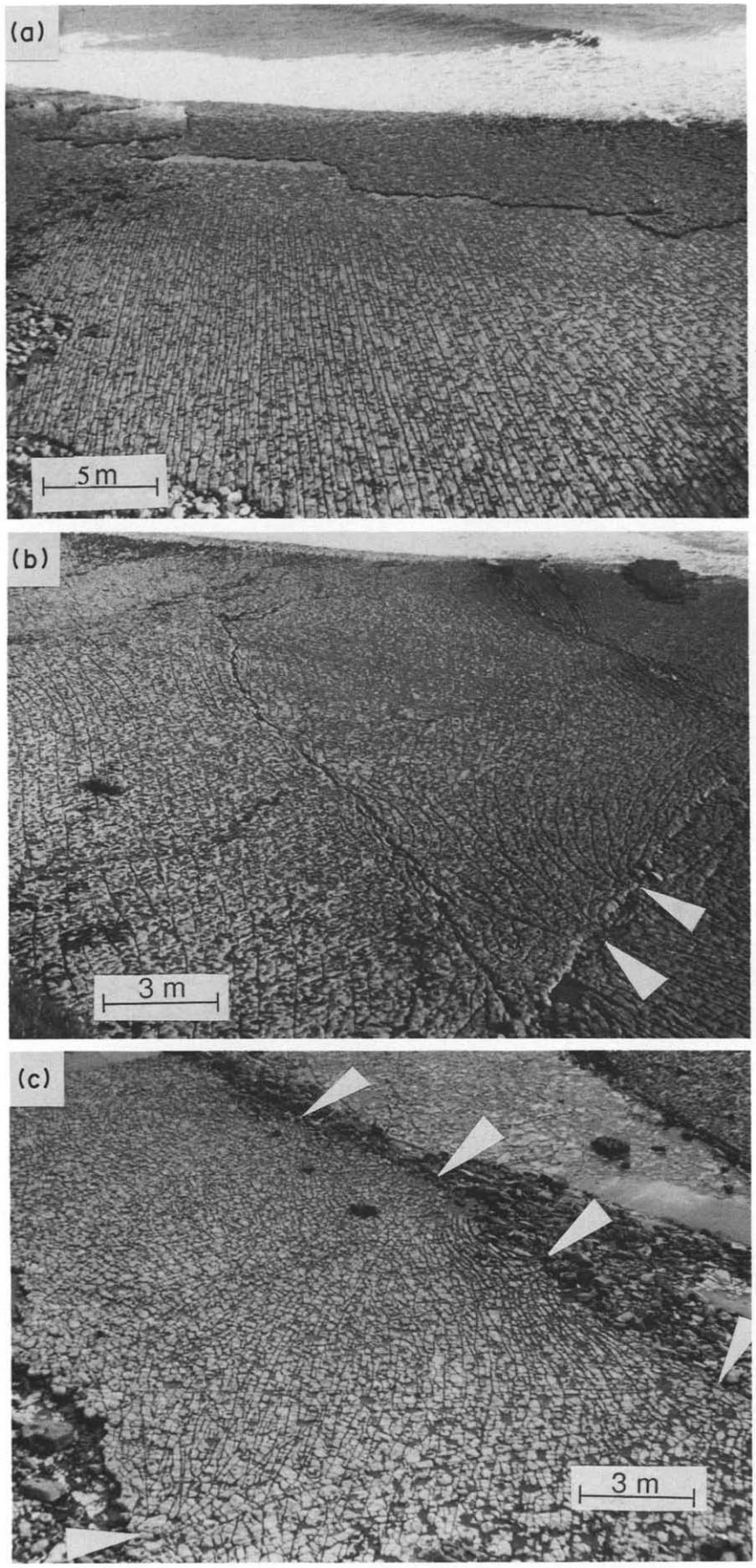

Fig. 2. Joint patterns of Nash Point. (a) A set of unperturbed linear fractures strikes 170° and is spaced 0.3 m. Orthogonal joints rarely cross-cut the 170° joints. (b) Simple perturbations around 010° and 160° faults, two points of joint convergence are indicated on a 010° fault. Joints to the left of view are relatively unperturbed and display a continuous curvature into the perturbed zones. (c) Complex perturbation with several points of joint convergence on adjacent faults. Joints are almost radial from each point creating a polygonal (and in some places rhombic) joint pattern. All views are towards 180°.

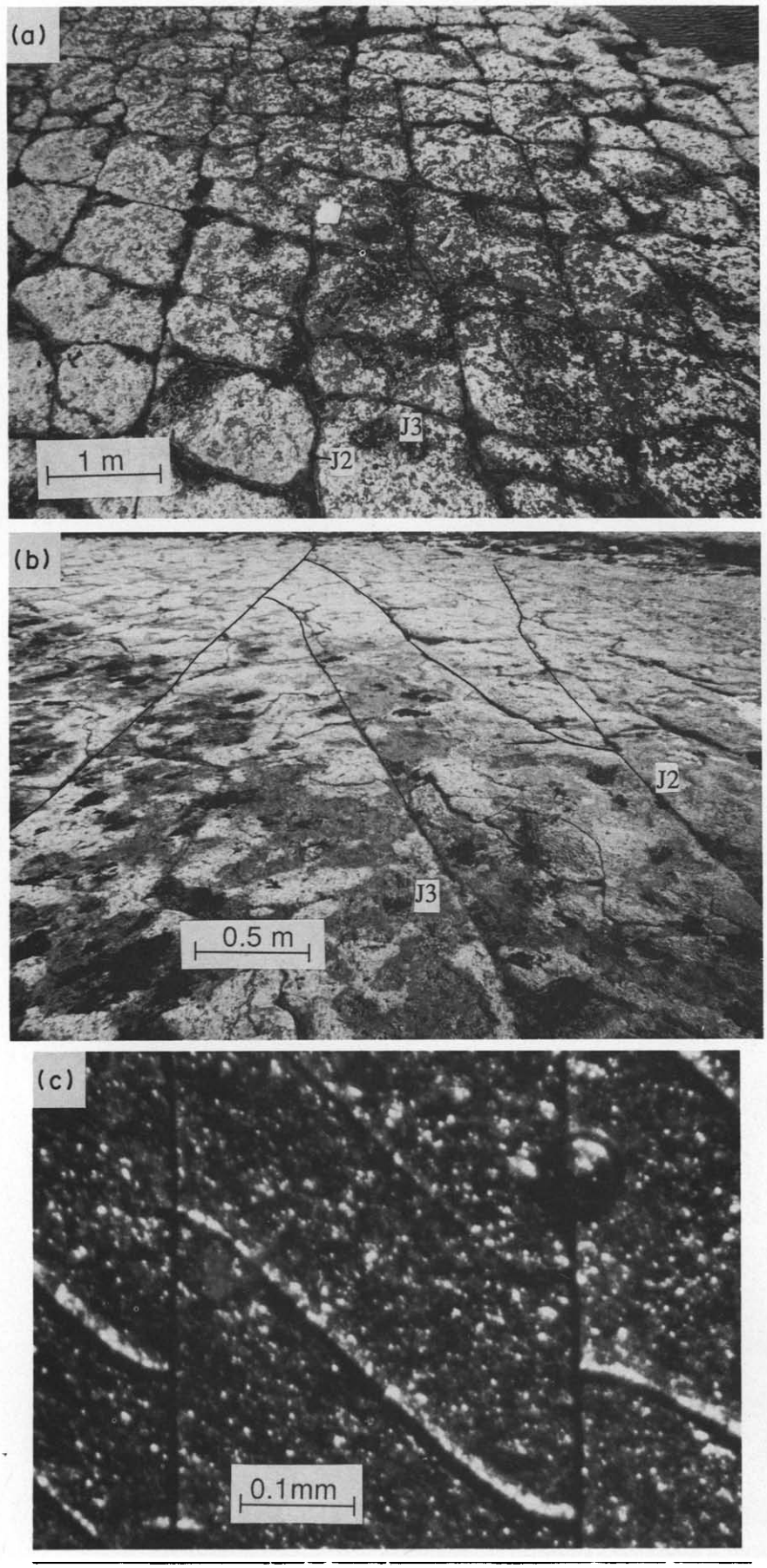

Fig. 4. (a) & (b) Joint patterns at Robin Hood's Bay (Yorkshire coast, U.K.). (a) Location 5 showing rhombic joint pattern. View towards 180°. (b) Location 8, set J_2 strikes 160° and shows linear and parallel geometry (spacing is approximately 4 m). Set J_3 strikes 120° and curves to become perpendicular to set J_2. View towards 160°. (c) Analogue fracture pattern in brittle varnish, initial set linear and parallel, second set oblique with curving perpendicular geometries.

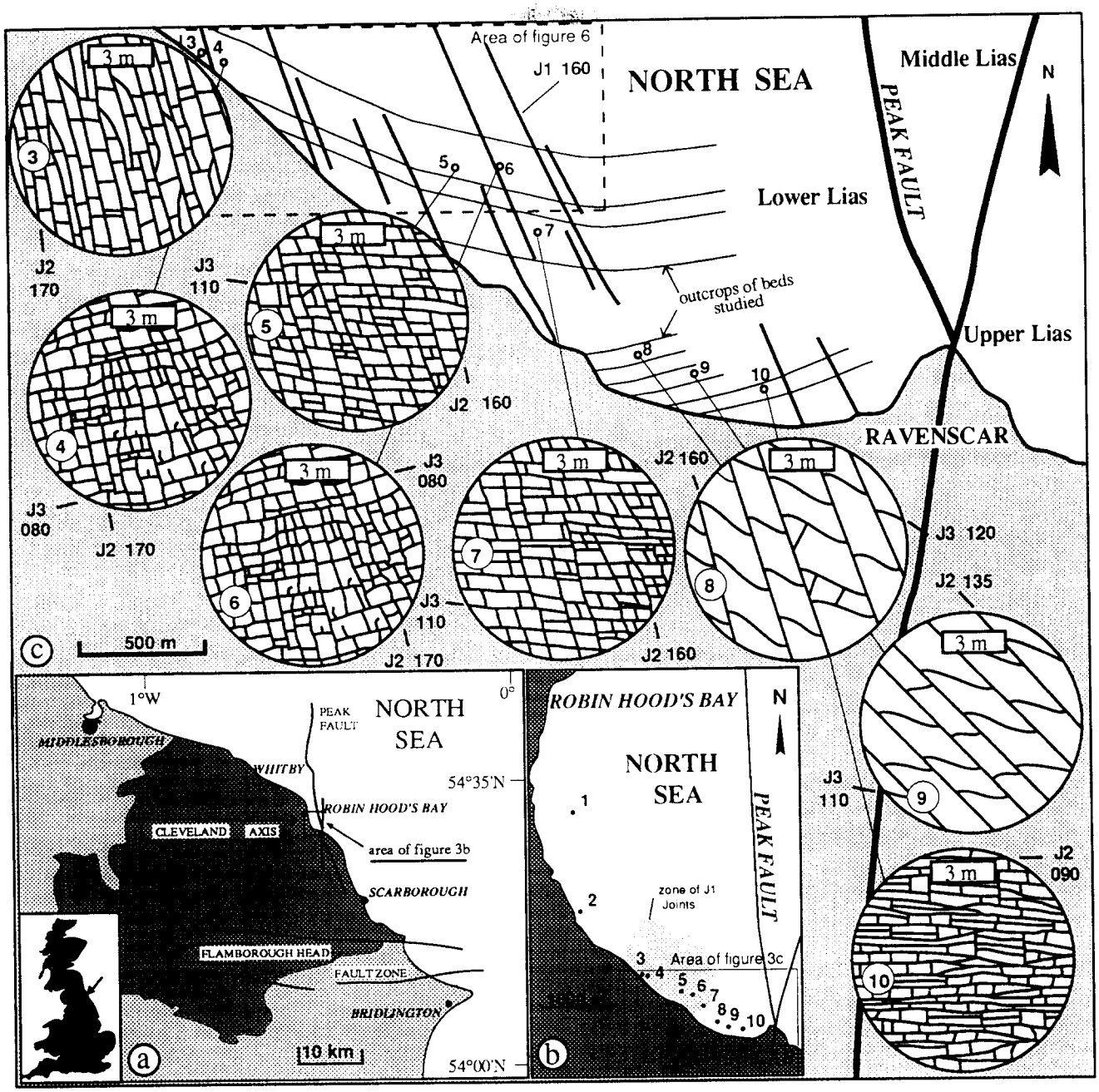

Fig. 3. (a) Geographical location and geological setting of Robin Hood's Bay (Yorkshire coast, U.K.). The dark stippled area is Jurassic outcrop. (b) Position of locations 1–10 around Robin Hood's Bay. The zone in which the J_1 joints are concentrated is indicated. (c) Detail of the area between location 3 and the Peak Fault. The position of each J_1 joint is indicated. Schematic details of the joint patterns at locations 3–10 are presented in inset circles which are connected by a line to the position where the joint pattern is exposed. Locations 3–6 are on the same bedding surface.

The dome is part of the E–W-trending axis of the Cleveland Anticline which can be traced for many kilometres to the west of the bay with gentle dips both to the north and south. The Cleveland Anticline is related to N–S Tertiary compression (Kirby *et al.* 1987) which uplifted the Lower Lias from a maximum burial depth of between approximately 1.7 km (a minimum value from extrapolation of overlying sediments, P. Bentham 1990, personal communication) and 2.5 km (Hemingway & Riddler 1982, from geochemical analysis). The dome is truncated to the east by the N–S-trending Peak Fault (Fig. 3) which downthrows Upper Lias sediment to the east, with a vertical throw of between 120 and 150 m (Fox-Strangways & Barrow 1915). Analysis of recent seismic sections (Milson & Rawson 1989) and field studies (Alexander 1986) reveals that the Peak Fault forms the western border of a faulted sedimentary trough, some 30 km long and 5 km wide. The Peak Fault has been active since the Triassic with further movements during the mid- to late-Jurassic (or early Cretaceous) and again during early Tertiary compression, with the latter possibly involving strike slip motion (Hemingway & Riddler 1982). The Ravenscar peninsula corresponds to a fork in the Peak Fault which now exposes a small block of Middle Liassic. The joint pattern at Robin Hood's Bay has attracted previous

attention (see Attewell & Taylor 1971); however the perturbation due to the fault has not been considered.

Robin Hood's Bay: joint network

The joint pattern systematically changes with decreasing distance to the Peak Fault (Fig. 3c). Joint traces exposed on the surfaces of the resistant calcareous–siliceous beds are described at 10 representative locations along a traverse towards the fault (Fig. 3b; e.g. Figs. 4a & b). Locations 3–6 are within the same bed. The surface features of the joint planes are unexposed and as a result propagation directions cannot be determined by fractographic analysis.

In aerial photographs of Robin Hood's Bay at a scale of 1:10,000 several large-scale joints striking 160° are observed (set J_1, Fig. 3c), some with horizontal trace lengths of over 300 m. At outcrop, the traces of the J_1 'joints' observed in the aerial photographs can be seen to be highly weathered zones of closely spaced joints. A vertical offset of approximately 5 cm is displayed by several J_1 zones. As this movement could easily be the result of differential subsidence, uplift or flexures to either side of the fracture plane, the term 'joint' is used in preference to 'fault'. Most of the J_1 traces are concentrated in an area around locations 3–7 (Fig. 3c). In cliff sections adjacent to location 3 the height of the J_1 joints is over 40 m.

The joint patterns at locations 1, 2 and 3 are similar. At each of these locations a set of vertical joints with horizontal trace lengths generally between 5 and 100 m is present (set J_2, Fig. 3c). This joint set is present, with slight changes in direction, along the coastline between Scarborough and Whitby, and is present in Liassic and Middle Jurassic sediments (Rives *et al.* 1992). At Robin Hood's Bay, the strike of J_2 changes gradually from 145° at stations 1 and 2, to 170° at location 3, and slightly oblique to the J_1 joints (J_2 joints at station 1 are shown in the fig. 1c of Attewell & Taylor 1971). Joints orthogonal to set J_2 are present at location 3 (set J_3, Fig. 3c). J_3 joints are vertical and usually abut against the nearest J_2 joints creating the 'rungs' of a ladder-like pattern on the surface of the bedding plane. Only a few J_3 joints cross-cut one or two J_2 joints before abutting. The J_3 joints often display a forking geometry before either abutting against or traversing the J_2 joints (Fig. 5a). The frequent abutments of J_3 against J_2 and the forking geometry of the J_3 joints when a J_2 joint is approached, indicates that J_3 is younger than J_2.

At location 4 the directions and characteristics of set J_2 and J_3 are the same as at location 3 (Figs. 3c and 5b) except that J_3 joints cross-cut a larger number of J_2 joints which creates a pattern of squares on the surface of the bedding plane.

Between locations 4 and 5, and on the same bedding surface as location 3, the 'square' pattern is gradually replaced by a 'rhombic' pattern (Figs. 3c, 4a, 5c and 6). At location 5 the strikes of set J_2 and J_3 are, respectively, 160° and 110°. Both sets have horizontal trace lengths between approximately 1 and 30 m. Set J_3 is less linear than J_2 (Fig. 5c) but is more linear than set J_3 at location 4 (Fig. 5b). The forking geometry displayed by J_3 joints when a J_2 joint is approached is less apparent than at location 4 (Figs. 4a and 5c). The rhombic pattern is present at all points on the bedding surface to the east of location 5, except for a tendency of J_3 to become orthogonal to J_1 within approximately 30 m of the latter (Fig. 6). The rhombic pattern is also present within overlying beds (e.g. location 7, Fig. 3c).

Location 8 is closer to the Peak Fault and displays a different joint pattern. Set J_2 strikes 160° and has horizontal trace lengths of over 30 m. At location 8 set J_3 is oblique to J_2 (striking 120°) and has a curving-perpendicular geometry at abutments with J_2 joints (Figs. 3c and 4b). Between locations 8 and 9 joint set J_2 curves progressively to 135° and set J_3 rotates anti-clockwise to 110°.

Between locations 9 and 10 set J_2 curves to become E–W (Fig. 3c). At location 10 set J_3 is either not present or is parallel to J_2. From location 10 to the Peak Fault the strike of set J_2 does not change.

To summarize the joint pattern at Robin Hood's Bay, set J_1 is a widely spaced set with horizontal trace lengths commonly over 300 m with a near constant strike of 160° not influenced by the Peak Fault. Set J_2 has horizontal trace lengths normally between 5 and 100 m. The strike of set J_2 is 145° in the northwest of the bay and rotates clockwise to 170° in the area of J_1 concentration. Closer to the Peak Fault set J_2 rotates anti-clockwise from 170° to 090°. The perturbation in the direction of set J_2 by J_1 indicates that set J_2 is younger. Set J_3 has horizontal trace lengths generally between 1 and 30 m. Set J_3 strikes mostly 110° except in the vicinity of a J_1 joint where J_3 joints curve to become perpendicular to the J_1 joint. Between locations 8 and 9 the strike of set J_3 rotates slightly anti-clockwise. At location 10 set J_3 is absent or sub-parallel to J_2. The interactions (abutments, forking and curving perpendicular geometries) indicate that J_3 is younger than J_2.

REGIONAL DIRECTIONS OF THE MAXIMUM HORIZONTAL STRESS

In order to interpret local stress field perturbations it is necessary to identify the regional (or remote) unperturbed directions of the principal stresses at the time of joint formation. The strike of a regional joint set, with a constant direction, is parallel to the maximum regional horizontal stress and is therefore the direction of either σ_1 or σ_2 (provided that one principal stress is vertical).

Nash Point

The regional direction of the joints at Nash Point is approximately 170° indicating that σ_H had the same direction. Because the orthogonal set does not cross-cut the 170° joints it is probably the result of relaxation phenomena and does not represent a separate regional stress event (Nickelsen & Hough 1967, Rives & Petit

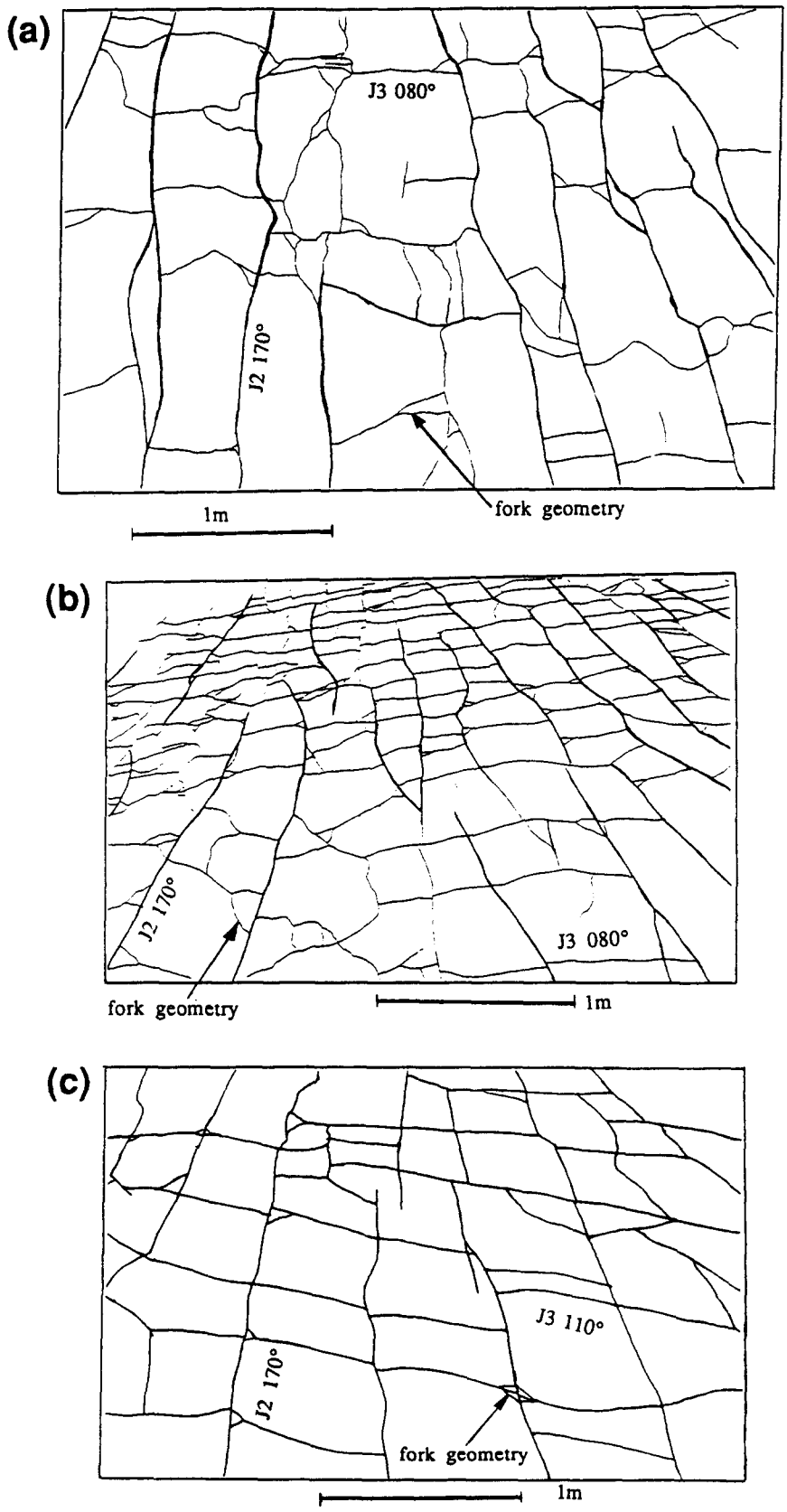

Fig. 5. Details of the joint pattern exposed on bedding surfaces at Robin Hood's Bay. (a) Location 3, ladder pattern. (b) Location 4, orthogonal pattern. (c) Location 5, rhombic pattern (see Fig. 4a). All views are drawn from photographs, (a) is a view vertically downwards, (b) and (c) are views towards the north.

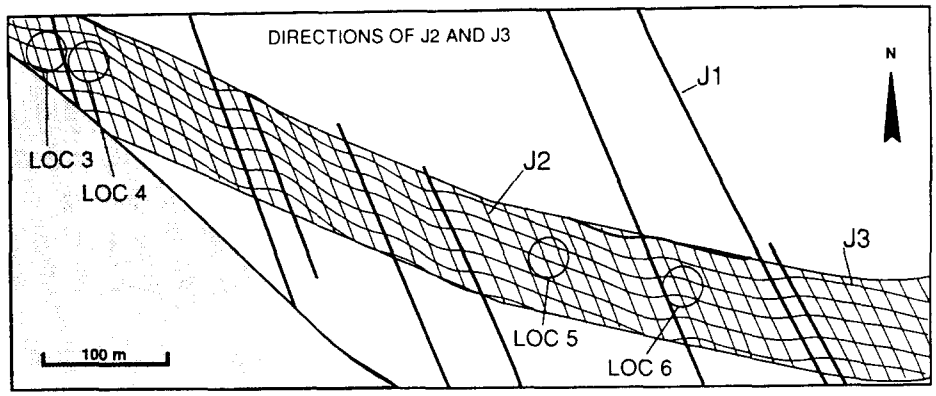

Fig. 6. Lines following the strikes of sets J_2 and J_3 on the bedding surface between locations 3 and 6. The positions of the J_1 joints are indicated. In the vicinity of a J_1 joint sets J_2 and J_3 are orthogonal. At a distance from J_1 joints J_2 and J_3 form a rhombic pattern.

1990a, b). The points of joint convergence along the fault planes indicate local perturbations of this regional stress field.

Robin Hood's Bay

Set J_1 strikes approximately 160° and shows no change in direction towards the Peak Fault, indicating that the direction of the regional maximum horizontal stress during the formation of set J_1 (σ_{HJ_1}) was 160°. The constant 145° direction of the strike of set J_2 between locations 1 and 2 indicates that, at the scale of the bay, this was the regional direction of σ_H during the formation of set J_2 (σ_{HJ_2}). The regional direction of σ_H during the development of J_3 (σ_{HJ_3}) is not well constrained because the continuation of set J_3 to the west and north of location 4 and to the east of location 9 is uncertain. At location 3 the J_3 joints could be the result of purely relaxation phenomena as they only rarely cross-cut the J_2 joints (Nickelsen & Hough 1967, Rives & Petit 1990a, b). The curvature of J_2 towards the Peak fault and more local deviations of J_2 and J_3 indicate perturbations of the remote stress fields.

MODELS FOR STRESS FIELD PERTURBATION AT FAULTS

The observed local joint pattern deviations, with respect to σ_H, at the described exposures could be explained with reference to two models of stress field perturbation in the vicinity of fractures.

Point of stress concentration model

It is well known from physical models of friction that the behaviour of the two surfaces in contact is best described by the existence of distinct points of contact, rather than an even contact along the interface (Kragelskii 1965). This applies even for apparently smooth fractures due to the inability of the two surfaces to meet exactly. Increasing normal stress applied across the fracture only enlarges the existing points of contact and creates new points but does not completely close the fracture (Bandis *et al.* 1981). The stress transmitted across the fracture surface is therefore concentrated at these points causing a spatial perturbation in the stress field. Points of high stress concentration may act as Hertzian indentors, which can produce diverging isostatics (Lawn & Wilshaw 1975a, b, Lindqvist 1984, Mouginot & Maugis 1985). A photo-elastic study of the stress state close to simulated rock fractures (Hyett & Hudson 1990) has shown the stress concentration at points along a typical fracture surface. Hyett (1990) indicated that decreasing the number of contact points, for example by offsetting the fracture surfaces from their mated condition, increases the stress concentration at each point, thereby increasing the size of the perturbed zones. From a photo-elastic study of a fracture surface with distinct points of contact, the stress trajectories are found to converge towards the points (work in progress, Fig. 7). As joints follow the stress trajectories they will converge at each point of contact.

A related mechanism (Fig. 8) occurs when points of high friction on a fault plane (a step or other barrier) restrain lateral movement of the fault and therefore concentrate stress. During reactivation or propagation of rock fractures such stress point concentrations are common (Jaeger & Cook 1979, Segall & Pollard 1980, Liu 1983) and can perturb the stress field in the adjacent rock.

Joints following the perturbed stress trajectories can be expected to curve towards points of stress concentration on fault planes.

Free surface model

Elastic analysis of the stress field at an existing open fracture of height $2c$ (Fig. 9) and infinite length in an otherwise homogeneous, infinite body indicates that one of the principal stresses must be perpendicular to the free surface and have zero magnitude. For remote stresses inclined to the free surface this requires a rotation of the principal stresses and a decrease in the magnitude of at least one principal stress. Joints following the stress trajectories can curve to become parallel or perpendicular to the free surface.

In the analysis of Dyer (1988) σ_1 is vertical, $\sigma_3 = -1\sigma_t$

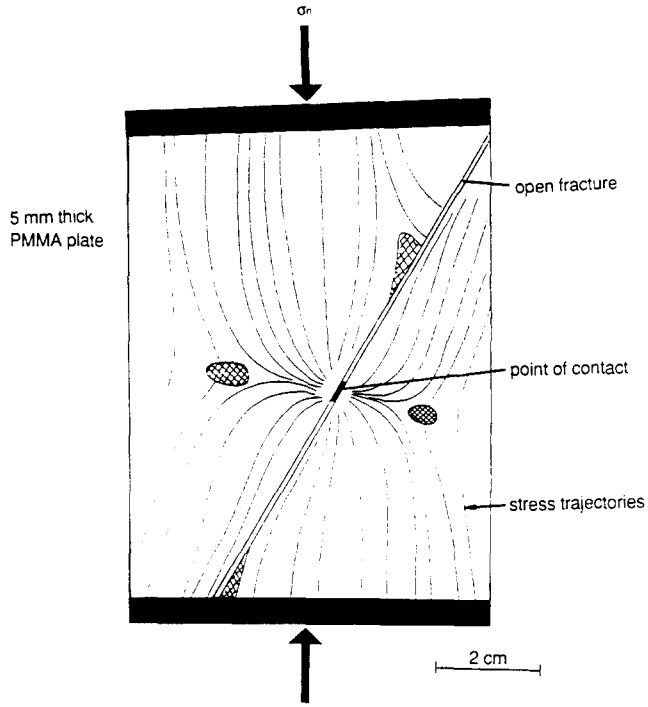

Fig. 7. Photo-elastic study of the stress trajectories about a single point of contact on a fracture surface inclined with respect to the applied stress. The photo-elastic plate (PMMA) contains a pre-existing discontinuity within which a relatively small section of metal is inserted to represent a distinct point of contact between the two surfaces. The plate is uniaxially loaded in a compression cell. Stress concentrates at points of contact causing the stress trajectories to converge towards them. The shaded areas correspond to regions of isotropic stress. The size of the perturbed zones, relative to the size of the fractures may be many times greater than that illustrated (see also Hyett & Hudson 1990).

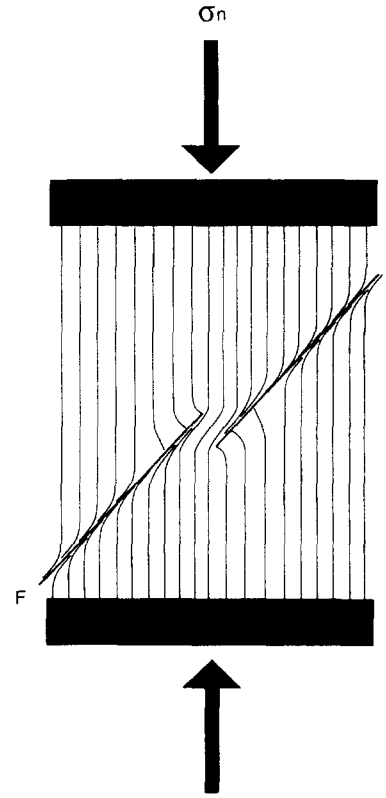

Fig. 8. Deviations of the major principal stress direction linked to the presence of a fault (F) deduced from micro-structures and mathematical modelling. The compressive relay zone constitutes a stress concentration zone (from Liu 1983).

for joint propagation (where σ_t is the tensile strength of the rock, considered as the 'unit tension'), and the angle τ between the free surface and the remote maximum horizontal stress is 30° ($\sigma_H = \sigma_2$). For a uniform fluid pressure P in the rock, joint propagation will occur providing that $\sigma_3 - P = -1\sigma_t$. The existing fracture will remain open and act as a free surface providing that the normal stress at the fracture surface is zero or tensile (σ_{yy} in the analysis of Dyer) (Fig. 9). For the specified geometry and stress condition σ_{yy} is zero or tensile for the range $-1\sigma_t < \sigma_2 < 3\sigma_t$. A joint propagating towards an open fracture is predicted to show curving-perpendicular geometry if the horizontal stress parallel to the free surface is tensile (σ_{zz} in the analysis of Dyer) which requires $-1\sigma_t < \sigma_2 < 1/3\sigma_t$. If σ_2 is greater than $1/3\sigma_t$, σ_{zz} is compressive and curving-parallel geometry is expected provided the fracture remains open (i.e. $1/3\sigma_t < \sigma_2 < 3\sigma_t$). At $\sigma_2 > 3\sigma_t$ the normal stress σ_{yy} at the free surface is compressive and the fracture is assumed to be closed. Under the closed condition, with or without frictional sliding, the stress field perturbation is such that a joint propagating towards the existing fracture would enter a zone in which σ_3 is compressive and further joint propagation would be inhibited.

Following Dyer (1988) the size of the perturbed zone around an open vertical fracture is proportional to its height. Curving-perpendicular geometry is expected to occur at a distance of $y/c \approx 0.2$, where y is the normal

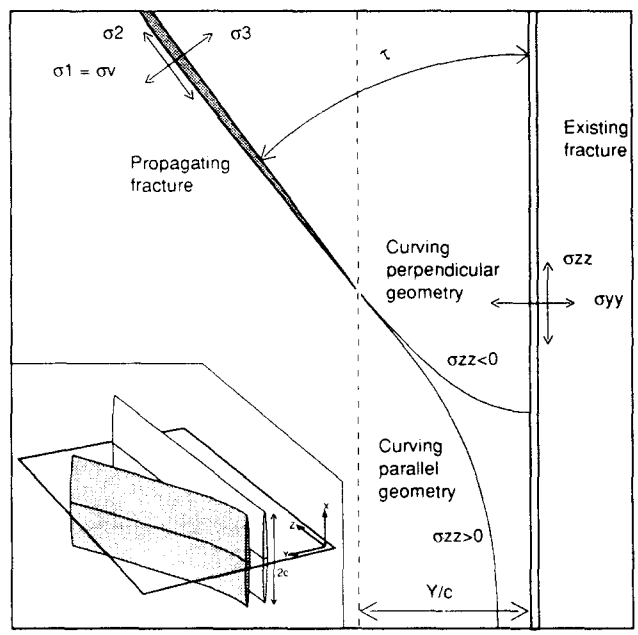

Fig. 9. Parameters employed in the free surface model of Dyer (1988). Idealization of the existing joint as an infinitely long crack of height $2c$. The z-axis is horizontal and parallel to the crack, the y-axis is perpendicular to the crack and the x-axis is vertical. The crack is subjected to far field stresses in the horizontal plane (σ_3 and σ_2). σ_1 is vertical and co-linear with the x-axis. τ is the angle between σ_2 and the z-axis. The resolved stresses on the crack are σ_{xx}, σ_{yy} and σ_{zz}. A second crack propagating towards the existing crack follows the direction of σ_2. Curving perpendicular is predicted for $\sigma_{zz} < 0$ and curving parallel for $\sigma_{zz} > 0$.

distance from the free surface. Curving-parallel geometry is expected to occur at a larger distance $y/c \approx 0.6$ (inferred from Dyer's fig. 12). Dyer does not consider the interaction between the growing joint and the pre-existing joint and as a result the analysis is described as a 'first approximation' to the true state.

Rives (1991) created curving-perpendicular (Fig. 4c) and curving-parallel geometries with fractures in a brittle varnish coating following (i) initial traction creating linear parallel fractures, and (ii) a second traction direction 45° anti-clockwise from the first. The second direction induces fractures at 45° to the first fractures which act as free surfaces in the brittle coating. As the new fractures propagate towards the existing fractures they curve to become perpendicular to and finally abut against initial fractures. In this model σ_1 is vertical and approximately zero, and $-1\sigma_t < \sigma_2 < 0$. Varying the angle τ between first and second fractures it was found that above a critical angle of approximately 20° curving-parallel geometry is replaced by curving-perpendicular geometry.

In the analogue model, the fractures are open at the surface and sealed at depth. The perturbation size for curving perpendicular geometry ($y/c > 10$) is much greater than that predicted by Dyer (1988; $y/c = 0.2$) for free surfaces closed both above and below in an infinite medium. The greater size of the perturbed zone in the analogue model can be explained intuitively by the absence of elastic restraint above the existing fracture, so allowing greater perturbation. The analogue model may therefore correspond more closely to the perturbation around a fault which cuts the Earth's surface, than a joint contained within the rock.

APPLICATION OF THE PERTURBATION MODELS

Nash Point—stress concentration model

The continuity of the joints from the regional unperturbed set to strongly perturbed zones in the vicinity of faults indicates that the joint pattern reflects a perturbation of the regional stress field. The points of joint convergence along the fault planes are not consistent with the free surface model as the joint pattern does not show systematic curving-parallel or -perpendicular geometries. The joint pattern is more easily explained by the points of stress concentration model. In this model the regional stress trajectories (striking 170°) locally converge to points of stress contact on the fault planes. The strike-slip faults at Nash Point could correspond to the un-mated fracture condition of Hyett & Hudson (1990) with high stress concentrations at relatively few points of contact (Fig. 2b). The resulting joints converge towards the points of stress concentration. Many adjacent points of convergence could produce the complex superpositions of the converging joints observed at Nash Point between closely spaced faults (Fig. 2c). Although it appears that the joint pattern developed within a relatively short time, the detailed sequence of joint development in such situations can be very complex.

Robin Hood's Bay—the free surface model for J_2

The joint pattern at Robin Hood's Bay displays complex variations. Set J_1 is unperturbed whereas set J_2 displays a large-scale curvature towards the Peak Fault. In this section we try to interpret the curvature of set J_2 joint pattern in terms of the previously described free surface model. The angle between the regional direction of σ_H during the formation of set J_2 (σ_{HJ_2}) and the Peak Fault was approximately 35°. Set J_2 curves to become perpendicular to the Peak Fault over a distance of approximately 1 km (Fig. 3). If the curvature of set J_2 is due to a stress field perturbation the effective remote stress condition could have been $\sigma_3 = -1\sigma_t$, $-1 < \sigma_{2J_2} < 1/3\sigma_t$ and σ_1 vertical. Following Dyer's conclusion that at $\tau = 30°$, curving-perpendicular geometry will occur at a distance of $y/c \approx 0.20$ from the existing fracture, the vertical height over which the Peak Fault acted as a free surface during the formation of set J_2 must have been approximately 5 km. This would require near constant effective stress conditions throughout a 5 km thick sedimentary pile which is unrealistic. If the Peak Fault was open at the earth's surface and therefore more comparable to the analogue model (Fig. 4c), the height over which the fault was open may have been considerably less than 5 km and possibly only 100 m (if $y/c = 10$ as in the analogue model). The unperturbed direction of J_1 suggests that the Peak Fault was closed during the development of this set. During the later development of J_2 the Peak Fault was partially open and perturbed the stress field such that the direction of σ_H curves over approximately 1 km from 145° to become perpendicular to the fault. Set J_2 follows the curving-perpendicular stress trajectories (Fig. 10a).

In addition to its curvature towards the Peak Fault, set J_2 also curves towards parallelism with set J_1 in the area between locations 3 and 6 (Fig. 10b). In this area the angle τ between the regional direction of σ_{HJ_2} (145°) and J_1 (160°) was approximately 15°. Set J_2 curves gradually over a distance of approximately 500 m to become parallel to the J_1 joints in this area. The curving-parallel geometry is in agreement with the low τ.

Robin Hood's Bay—the point of stress concentration model for J_2

The point contact model for joint convergence at Nash Point can also be applied to set J_2 at Robin Hood's Bay. The curvature of set J_2 towards the fork in the Peak Fault could be due to a point of stress concentration at the fork (Fig. 11). The fault bifurcation at the Ravenscar peninsula could define a singular point of high stress concentration towards which the regional stress trajectories could converge. Set J_2 follows the isostatics and so converges towards the fault plane at the fork. At a smaller scale the interaction between sets J_1 and J_2 could

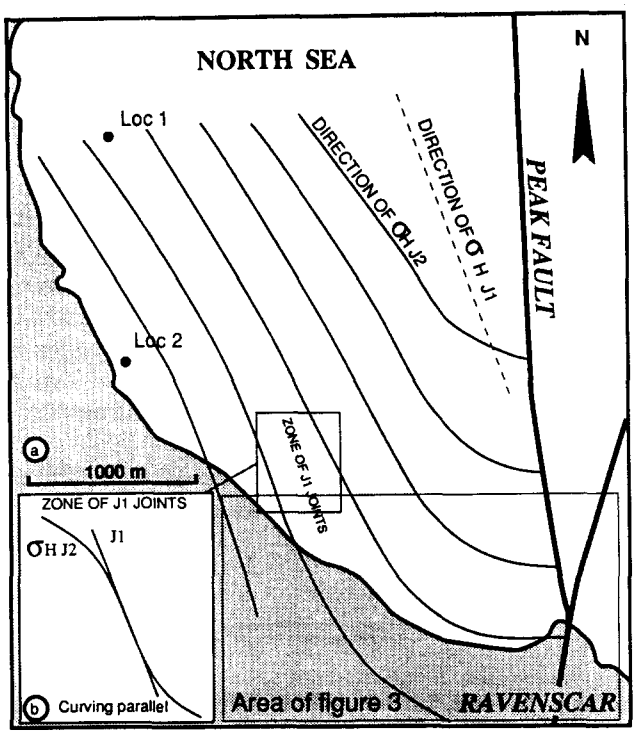

Fig. 10. Free surface model for the perturbation of the stress field during the formation of set J_2 at Robin Hood's Bay. The regional direction of the maximum horizontal stress is 145°. The Peak Fault is a free surface and perturbs the stress field such that the maximum horizontal stress curves to become perpendicular to the fault. Set J_2 follows the perturbed stress trajectories. Set J_1 joints are also free surfaces and perturb the stress field such that the maximum horizontal stress becomes locally parallel to them.

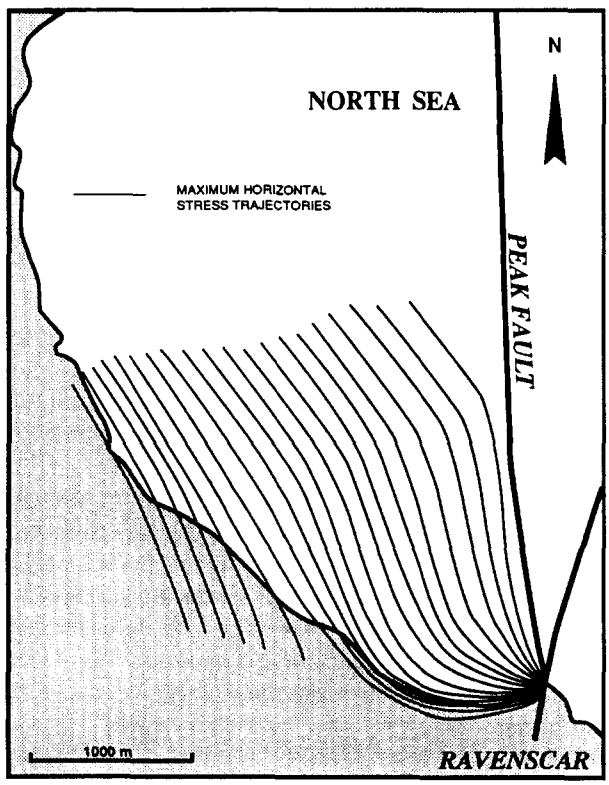

Fig. 11. Stress point concentration model for the perturbation of the stress field during the formation of set J_2, Robin Hood's Bay. The regional direction of the horizontal stress is 145°. Locally the direction of the maximum horizontal stress converges towards a point of high stress at the fork in the Peak Fault. Set J_2 forms parallel to the direction of the perturbed maximum horizontal stress.

be similar to that described above, assuming a free surface model.

Robin Hood's Bay—the development of J_3

Set J_3 is only clearly developed between locations 4 and 9 and although a slight anti-clockwise rotation in the direction of set J_3 is present between locations 8 and 9, this may not be the result of a stress field perturbation around the Peak Fault. The development of set J_3 is considered firstly at a metre scale and secondly at the kilometre scale of the bay.

At a small scale, the deviation in the direction of J_3 can be interpreted in terms of the free surface model. The free surface model is most clearly invoked for the curving-perpendicular geometry as J_3 joints approach J_2 joints at locations 8 and 9 (Fig. 4b). The value of τ is close to 30° (assuming that σ_2 is parallel to the strike of the linear sections of the J_3 joints at locations 8 and 9). Following Dyer (1988) this indicates that $\sigma_3 = -1\sigma_t$, $-1\sigma_t < \sigma_2 \leq 1/3\sigma_t$ and σ_1 was vertical during the formation of set J_3 (at locations 8 and 9). The height ($2c$) of the J_2 joints at locations 8 and 9 cannot be observed directly, but normally the horizontal traces cut two or three 1 m thick beds. If the joint height is equal to three beds ($c \approx 1.5$ m) the size of the perturbation, approximately 0.3 m, is in agreement with Dyer's analysis ($y/c \approx 0.2$). At a larger scale, set J_3 curves from 110° to 080° to become perpendicular to J_1 joints, (Fig. 3c). The high angle τ (60°) is in agreement with the curving perpendicular geometry. J_3 joints cross-cut several J_2 joints in the area between locations 4 and 6. This indicates that the magnitude of σ_{2J_3} was high enough to close J_2 joints but not high enough to close set J_1. This could be because each J_1 joint is a zone of tightly spaced parallel fractures that may require a greater normal stress to close completely.

The exposed strike of J_3 does not display a significant change in direction between locations 3 and 9. It is probable therefore that set J_3 is not perturbed by the Peak Fault (excluding the small-scale curvature of J_3 towards J_1 or J_2, the strike of J_3 varies only 10° between 110 and 120°). Because set J_3 is parallel to the strike of the beds, and sub-parallel to the axis of the Cleveland Anticline, this set could be related to a localized tensional stress perpendicular to the fold axis during the Tertiary compression. However it could be possible that set J_3 results from a similar perturbation of the regional stress field as required for J_2. In particular a secondary point of stress concentration may have developed further to the north of the exposed fault bifurcation resulting in a local anti-clockwise rotation of the stress trajectories and superimposing J_3 over J_2 (Fig. 12). However such a hypothesis remains speculative.

DISCUSSION OF THE JOINTING CONDITIONS

Nash Point

The regional joint strike and the acute bisector to the conjugate strike-slip faults are closely parallel to the

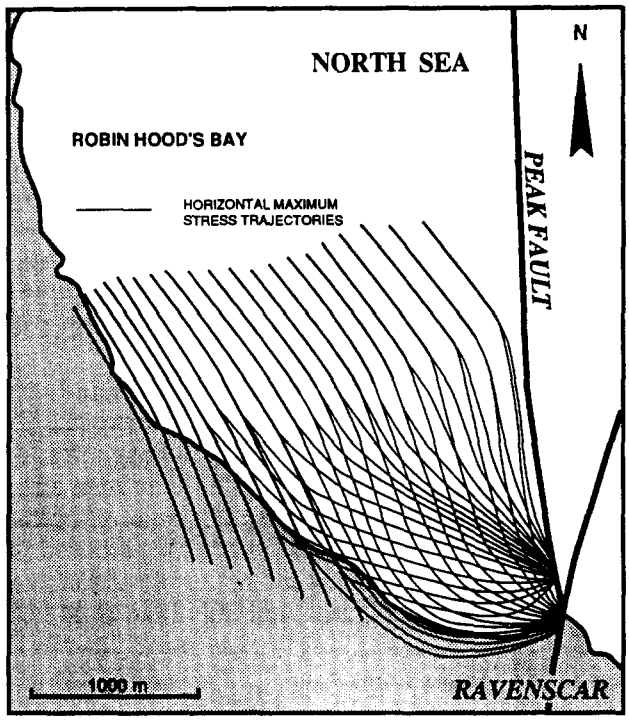

Fig. 12. Stress concentration model of the formation of sets J_2 and J_3, Robin Hood's Bay. The point of stress concentration at the bifurcation of the Peak Fault is the same as Fig. 11 and produces set J_2. Movement on the fault produces a second point of contact to the north. The stress trajectories converge at the second point. The stress magnitude decreases away from the fault. Set J_3 follows the perturbed stress trajectories. See text for details.

approximately N–S Tertiary compression direction. The regional joint set is strongly perturbed by the faults and is therefore syn- or post-faulting and probably Tertiary in age. The absence of an early and well-developed E–W joint set suggests that joint development did not occur during the late Jurassic or early Cretaceous N–S extension.

Robin Hood's Bay

Joint sets J_2 and J_3 display changes of direction towards, and may terminate against, existing joint sets. This indicates that sets J_1, J_2 and J_3 probably formed within a relatively short period of time, not sufficient for the joint walls of existing joints to be sealed or welded together. If the existing joints were sealed they may not have acted as free surfaces and have perturbed the stress field during the propagation of later joints.

The joint network at Robin Hood's Bay could be related to either Mesozoic E–W extension (North Sea rifting) or Tertiary N–S compression. At early stages of burial during the Jurassic it is possible that the Peak Fault was open to the Earth's surface, creating the conditions required for a free surface stress field perturbation. With increasing burial it becomes less probable that the Peak Fault remained open between the Lias horizon and the Earth's surface. Therefore if the joints are Jurassic in age then they must have formed at relatively shallow depths. The continuity of the joints throughout the Lower and Middle Jurassic (at Whitby and Scarborough) argues against the free surface model, as this would require the Peak Fault to have been connected to the surface after the deposition of the Middle Jurassic, a height of over 600 m.

During the Tertiary the effective normal stress on the fault plane was probably mostly compressive and compatible with the conditions required for the point of stress concentration model. The direction of the maximum horizontal stress would be approximately parallel to that of the joint set exposed between Scarborough and Whitby. The possibility that J_3 is related to the formation of the Cleveland Anticline is also compatible with a Tertiary age.

As a result a Tertiary age for the joints at Robin Hood's Bay is favoured by the authors.

CONCLUSIONS

Joint patterns can be perturbed in the vicinity of faults. Although the joint patterns appear complex, relatively simple models can be invoked to explain the development of the joints based on the analysis of perturbed stress fields.

At the two localities described, Nash Point and Robin Hood's Bay, a model based on the perturbation of the stress field due to stress concentration at points of contact along fault planes can help explain the observed joint patterns. In the proposed model, the local direction of the maximum horizontal stress is orientated towards each point. Joints follow the stress trajectories, and so converge at the points of contact. In places where there are closely spaced faults with adjacent points of convergence, the final joint pattern is the result of a complex superposition of the joints converging towards each point.

At Robin Hood's Bay a model based on the perturbation of the stress field around faults acting as free surfaces can explain various metre-scale patterns, in particular curving-perpendicular and -parallel geometries as existing joints are approached. At the scale of the Peak Fault the free surface model is problematic due to the unrealistic height over which the fault plane must be open.

In both of the examples the perturbations in the stress field are revealed only by the joints; other sensitive stress markers are absent. This indicates that joints can be used as markers of stress field perturbations around faults.

A future application of this work may be to consider the role of joint interpretation in seismic studies, both in terms of determining the directions of the stress field and indentifying 'barriers' or 'asperities' which prevent stable fault sliding.

Acknowledgements—The authors would like to thank: ELF Aquitaine; L'Institut Français du Pétrole and the Natural Environment Research Council for their funding of various aspects of this work and G. Caillet of ELF Aquitaine for his assistance. Reviews by M. R. Gross and K. M. Cruikshank greatly improved the manuscript.

REFERENCES

Alexander, J. 1986. Idealised flow models to predict alluvial sandstone body distribution in the Middle Jurassic Yorkshire Basin. *Mar. & Petrol. Geol.* **3**, 298–305.

Attewell, P. B. & Taylor, R. K. 1971. Jointing in Robin Hood's Bay, North Yorkshire coast, England. *Int. J. Rock. Mech. Min. Sci.* **8**, 477–481

Bandis, S., Lumsden, A. C. & Barton, N. R. 1981. Experimental studies of scale effects on the shear behaviour of rock joints. *Int. J. Rock Mech. & Mining Sci. & Geomech. Abs.* **18** 1–21.

Barquins, M. & Petit, J.-P. 1992. Kinetic instabilities during the propagation of a branch crack: effects of loading conditions and internal pressure. *J. Struct. Geol.* **14**, 893–903.

Brooks, M., Trayner, P. M. & Trimble, T. J. 1988. Mesozoic reactivation of Variscan thrusting in the Bristol Channel area, U.K. *J. geol. Soc. Lond.* **145**, 439–444.

Chadwick, R. A. 1986. Extension tectonics in the Wessex Basin, southern England. *J. geol. Soc. Lond.* **143**, 465–488.

Dyer, R. 1988. Using joint interactions to estimate paleostress ratios. *J. Struct. Geol.* **10**, 685–699.

Engelder, T. 1987. Joints and shear fractures in rock. In: *Fracture Mechanics of Rock* (edited by Atkinson, B. K.). London, Academic Press, 27–69.

Engelder, T. & Geiser, P. 1980. On the use of regional joint sets as trajectories of paleostress fields during the development of the Appalachian plateau, New York. *J. geophys. Res.* **85**, 6319–6341.

Engelder, T. & Lacazette, A. 1990. Natural hydraulic fracturing. In: *Rock Joints* (edited by Barton, N. & Stephansson, O). Balkema, Rotterdam, 35–43.

Fletcher, R. C. & Pollard, D. D. 1981. Anti-crack model for pressure solution surfaces. *Geology* **9**, 419–424.

Fox-Strangways, C. & Barrow, F. G. S. 1915. *The Geology of the Country Between Whitby and Scarborough. Mem. geol. Surv. Engl. & Wales.*

Hancock, P. L. 1985. Brittle microtectonics: principles and practice. *J. Struct. Geol.* **7**, 437–457.

Hemingway, J. E. & Riddler, G. P. 1982. Basin inversion in North Yorkshire. *Trans. Inst. Min. Metall.* **91**, B175–B186.

Holloway, S. & Chadwick, R. A. 1986. The Sticklepath—Lustleigh fault zone: Tertiary sinistral reactivation of a Variscan dextral strike-slip fault. *J. geol. Soc. Lond.* **143**, 447–452.

Hyett, A. I. 1990. The potential state of stress in a naturally fractured rock mass. Unpublished Ph.D. thesis, University of London.

Hyett, A. I. & Hudson, J. A. 1990. A photo-elastic investigation of the stress state close to rock joints. In: *Rock Joints* (edited by Barton, N. & Stephansson, O.). Balkema, Rotterdam, 227–233.

Jaeger, J. G. & Cook, N. G. 1979. *Fundamentals of Rock Mechanics.* Methuen, London.

Kazi, M. A. 1982. Deformation of Carboniferous Rocks in the Pennines. Unpublished Ph.D thesis, University of Leeds.

Kirby, G. A., Smith, K., Smith, N. J. P. & Swallow, P. W. 1987. Oil and gas generation in eastern England. In: *Petroleum Geology of North West Europe* (edited by Brooks, J. & Glennie, K.), 171–180.

Kragelskii, I. V. 1965. *Friction and Wear.* Butterworths, London.

Ladeira, F. L. & Price, N. J. 1981. Relationship between fracture spacing and bed thickness. *J. Struct. Geol.* **3**, 179–183.

Lawn, B. R. & Wilshaw, J. R. 1975a. *Fracture of Brittle Solids.* Cambridge University Press, Cambridge.

Lawn, B. R. & Wilshaw, J. R. 1975b. Review Indentation fracture: principles and applications. *J. Mater. Sci.* **10**, 1040–1081.

Lindqvist, P.-A. 1984. Stress field and subsurface crack propagation of single and multiple rock indentation and disc cutting. *Rock Mech. & Rock Engng* **17**, 97–112.

Liu, X. 1983. Perturbations de contraintes liées aux structures cassantes dans les calcaires fins du Languedoc. Observations et simulations mathématiques. Unpublished Thèse 3ème cycle, U.S.T.L., Montpellier.

Lorenz, J. C., Teufel, L. W. & Warpinski, N. R. 1991. Regional fractures I: A mechanism for the formation of regional fractures at depth in flat-lying reservoirs. *Bull. Am. Ass. Petrol. Geol.* **75**, 1714–1737.

Milson, J. & Rawson, P. F. 1989. The Peak Trough a major control on the geology of the North Yorkshire coast. *Geol. Mag.* **126**, 699–705.

Mouginot, R. & Maugis, D. 1985. Fracture indentation beneath flat and spherical punches. *J. Mater. Sci.* **20**, 4354–4376.

Narr, W. & Suppe, J. 1991. Joint spacing in sedimentary rocks. *J. Struct. Geol.* **13**, 1037–1048.

Nickelsen, R. P. & Hough, V. N. D. 1967. Jointing in the Appalachian plateau of Pennsylvania. *Bull. geol. Soc. Am.* **78**, 609–630.

Olson, J. & Pollard, D. D. 1989. Inferring paleostress from natural fracture patterns: A new method. *Geology* **17**, 345–348.

Pollard, D. D. & Aydin, A. 1988. Progress in understanding jointing over the past century. *Bull geol. Soc. Am.* **100**, 1181–1204.

Petit, J. P. & Barquins, M. 1990. Fault propagation in Mode II conditions: Comparison between experimental and mathematical models, applications to natural features. In: *Mechanics of Jointed and Faulted Rock* (edited by Rossmanith, H. P.). Balkema, Rotterdam, 213–220.

Reik, G. A. 1973. Joints, microfractures and residual strain in Cardium siltstone, South Ram River area, Alberta. Unpublished Ph.D. thesis, University of Toronto.

Rispoli, R. 1981. Stress fields about strike-slip faults inferred from stylolites and tension gashes. *Tectonophysics* **75**, T29–T36.

Rives, T. 1991. Modélisation analogique des réseaux de diaclases. Conséquences pour l'interprétation des réseaux naturels. Rapport IFP 38317.

Rives, T. & Petit, J.-P. 1990a. Experimental study of jointing during cylindrical and non-cylindrical folding. In: *Mechanics of Jointed and Faulted Rock* (edited by Rossmanith, H. P.). Balkema, Rotterdam, 205–211.

Rives, T. & Petit, J.-P. 1990b. Diaclases et plissement: une approche expérimentale. *C.r.Acad.Sci., Paris* **310**, 1115–1121.

Rives, T. & Petit, J.-P. 1991. Joint patterns and local stress field evolution during non-cylindrical folding: experimental and field data. *EUG VI, Terra Abs.* **3**, 79.

Rives, T., Razack, M., Petit, J.-P. & Rawnsley, K. D. 1992. Joint spacing: analogue and numerical simulations. *J. Struct. Geol.* **14**, 925–937.

Roberts, D. G. 1989. Basin inversion in and around the British Isles. In: *Inversion Tectonics* (edited by Cooper, M. A. & Williams, G. D.). *Spec. Publ. geol. Soc. Lond.* **44**, 131–150.

Secor, D. T. 1965. Role of fluid pressure in jointing. *Am. J. Sci.* **263**, 633–646.

Segall, P. & Pollard, D. 1980. Mechanics of discontinuous faults. *J. geophys. Res.* **85**, 4337–4350.

Simon, J. L., Seron, F. J. & Casas, A. M. 1988. Stress deflection and fracture development in a multidirectional extension regime. Mathematical and experimental approach with field examples. *Annales Tectonicæ* **2**, 21–32.

Suppe, J. 1985. *Principles of Structural Geology.* Prentice-Hall, Englewood Cliffs, New Jersey.

Stoneley, R. 1982. The structural development of the Wessex Basin. *J. geol. Soc. Lond.* **139**, 543–554.

Van Hoorn, B. 1987. Structural evolution, timing and tectonic style of the Sole Pit inversion. *Tectonophysics* **137**, 239–284.

Wu, H. & Pollard, D. D. 1991. Fracture spacing, density, and distribution in layered rock masses: Results from a new experimental technique. In: *Rock Mechanics as a Multidisciplinary Science* (edited by Roegiers, J.-C.). Balkema, Rotterdam, 1175–1184.